

AD-A077 669

NAVAL RESEARCH LAB WASHINGTON DC
MECHANICAL PROPERTIES OF WROUGHT IRON
NOV 79 C D BEACHEM , D A MEYN , R A
NRL-MR-4123

F/G 20/11
ROM HULL PLATE OF USS MO--ETC(U)
YLES

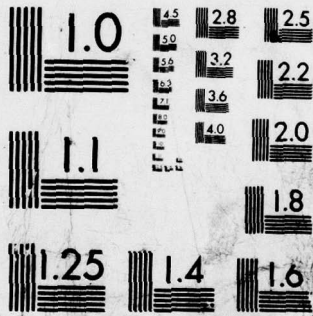
UNCLASSIFIED

NL

| OF |
AD
A077669



END
DATE
FILMED
2-79
-00C



MICROCOPY RESOLUTION TEST CHART
NATIONAL BUREAU OF STANDARDS-1963-A

12
B 5

NRL Memorandum Report 4123

AD A 077669

Mechanical Properties of Wrought Iron from Hull Plate of USS MONITOR

C. D. BEACHEM, D. A. MEYN, AND R. A. BAYLES

*Advanced Materials Technology Branch
Materials Science and Technology Division*

LEVEL II

November 20, 1979

DDC FILE COPY



DDC
RECEIVED
DEC 6 1979
A

NAVAL RESEARCH LABORATORY
Washington, D.C.

Approved for public release; distribution unlimited.

79 12 6 011

9 Memorandum repts,

SECURITY CLASSIFICATION OF THIS PAGE (When Data Entered)

REPORT DOCUMENTATION PAGE		READ INSTRUCTIONS BEFORE COMPLETING FORM
1. REPORT NUMBER NRL Memorandum Report 4123	2. GOVT ACCESSION NO.	3. RECIPIENT'S CATALOG NUMBER
4. TITLE (and Subtitle) MECHANICAL PROPERTIES OF WROUGHT IRON FROM HULL PLATE OF USS MONITOR	5. TYPE OF REPORT & PERIOD COVERED Topical report on a continuing NRL problem.	
	6. PERFORMING ORG. REPORT NUMBER	
7. AUTHOR(s) C. D/Beachem, D. A./Meyn and R. A./Bayles†	8. CONTRACT OR GRANT NUMBER(s) RR022-01-46	
9. PERFORMING ORGANIZATION NAME AND ADDRESS Naval Research Laboratory Washington, DC 20375	10. PROGRAM ELEMENT, PROJECT, TASK AREA & WORK UNIT NUMBERS 61153N-22	
11. CONTROLLING OFFICE NAME AND ADDRESS Office of Naval Research Washington, DC	12. REPORT DATE November 20, 1979	
14. MONITORING AGENCY NAME & ADDRESS (if different from Controlling Office) 14 NRL-MR-4123	13. NUMBER OF PAGES 18	
	15. SECURITY CLASS. (of this report) UNCLASSIFIED	
16. DISTRIBUTION STATEMENT (of this Report) Approved for public release; distribution unlimited.	15a. DECLASSIFICATION/DOWNGRADING SCHEDULE	
	17 RR0220146	
17. DISTRIBUTION STATEMENT (of the abstract entered in Block 20, if different from Report) 11 20 Nov 79 12 19	Accession For NTIS GRA&I <input checked="" type="checkbox"/> DDC TAB <input type="checkbox"/> Unannounced <input type="checkbox"/> Justification <input type="checkbox"/>	
18. SUPPLEMENTARY NOTES *National Research Council Resident Research Associate	By _____ Distribution/ Availability Codes	
19. KEY WORDS (Continue on reverse side if necessary and identify by block number) Mechanical properties USS Monitor Wrought iron Seawater corrosion Ductile-to-brittle transition	Dist. A	Avail and/or special
20. ABSTRACT (Continue on reverse side if necessary and identify by block number) Tensile tests of four specimens cut from a piece of hull plate recovered from USS Monitor reveal strength comparable to modern wrought iron except in the case of one specimen which suffered from internal corrosion. Impact tests and subsequent scanning electron fractography indicate that no ductile-to-brittle transition occurs until the temperature has been lowered to well below the temperature of the seawater at the site of the wreck.		

DD FORM 1 JAN 73 1473 EDITION OF 1 NOV 65 IS OBSOLETE S/N 0102-014-6601

SECURITY CLASSIFICATION OF THIS PAGE (When Data Entered)

251 950

JQB

The iron gunboat, USS Monitor, which sank in a storm off the coast of North Carolina on 31 December 1862 was discovered in August 1973 in 220 feet of water 16.1 miles south-southeast of Cape Hatteras.

The North Carolina Department of Cultural Resources in conjunction with the National Oceanic and Atmospheric Administration and other interested organizations is studying the feasibility of recovering the vessel.

The purpose of the work reported here is to determine the mechanical properties of samples from a hull plate recovered from the wreck in August 1977 and to study the microstructure of the plate to provide insight into the nature of wrought iron produced more than a century ago. The mechanical properties of the plate can provide valuable information about the loads which the structure will be able to withstand during the recovery operation. These studies may indicate the presence of insidious defects which may weaken the structure.

Prior to studying the metal which comprises much of the samples, a piece of the rust and accretion which covered the metal was examined. The primary constituents of the piece were rust, barnacle-like encrustations, a black, waxy material, and silicate particles. The latter are usual constituents of wrought iron. Figure 1 shows the rust piece which is typical of the coating of the plate. Figure 2 shows the layers of rust, wax, and barnacles. Figure 3 shows a two phase silicate particle embedded in the rust.

Of the four rectangular pieces of the hull plate received for study, two were too severely corroded to provide convenient sized tensile test specimens. The two other pieces, labeled 0404 and 0405, had large areas in which the thickness of the metal under the rust appeared to be greater than 2.5 mm (0.098 inch). Three strips 115 mm x 13 mm (4 1/2 x 1/2 inch) were cut from each of these two pieces. Each strip was placed in a separate labeled envelope for identification. The strips were machined to the dimensions of tensile test specimens as drawn in Figure 4. The thicknesses were approximately 2.3 mm (0.091 inch). One specimen had a narrower gage width and another was thinner in order to remove large corrosion pits from the specimen surface. Small pits were still evident on the specimen surfaces as shown in Figure 5. After machining, the specimens were surface-ground parallel to their long axes to obtain a uniform thickness along the length of each specimen. Two specimens from each of the two pieces were tested by pulling in a tensile testing machine at a constant cross-head speed of 21 $\mu\text{m/s}$ (0.050 inch/minute) until they fractured. The test machine measured and plotted the load as a function of specimen extension. The load was measured with a load cell and the extension was measured by an extensometer which was attached to the specimen. The mechanical properties obtained from the four specimens are the elastic modulus, E ; the yield strength at 0.2% strain, σ_y ; the ultimate strength, σ_u ; the elongation, e ; and the reduction of area, ΔA . The values determined by analysis of the load-extension curves are reported in Table I.

All four specimens exhibited a woody fracture surface and 0404A also exhibited severe delamination. The delaminated surfaces were flat and had rust-colored patches. Flat fracture surfaces on an otherwise ductile material indicate internal corrosion. Each of the eight fracture surfaces was studied in a

Note: Manuscript submitted September 18, 1979.

Table 1. Mechanical Properties of Wrought Iron from USS Monitor

	0404A	0404B	0405A	0405C
E		160GPa (23.2Mpsi)	192GPa (27.8Mpsi)	209GPa (30.3Mpsi)
σ_y	uncertain	198MPa (28.7ksi)	205MPa (29.7ksi)	205MPa (29.7ksi)
σ_u	110MPa (16.0ksi) 130MPa (18.9ksi)	265MPa (38.4ksi)	296MPa (42.9ksi)	297MPa (43.1ksi)
e	2.9%	5.7%	9.2%	15.9%
ΔA	6.0%	6.4%	15.0%	12.6%

high resolution scanning electron microscope. Figure 6 shows a typical woody fracture surface and Figure 7 shows the flat delamination surface. At higher magnifications the fracture surface is composed of dimpled and flat surfaces indicating a combination of microvoid coalescence around inclusion particles, ductile tearing, and shear. The inclusion particles are silicates in the form of spheres and platelets. These silicates probably form much of the debris observed on the surface. Figures 8 and 9 are micrographs of typical fracture surfaces and Figure 10 shows an area of the delaminated surface. Two large silicate platelets lie on the delaminated fracture surface. At higher magnification, in Figure 11, is seen the two phase nature of these particular platelets. Note that the secondary crack passes straight through an embedded particle indicating good bonding at the interface between the particle and the surrounding silicate. Electron/x-ray spectrometry indicates that the small nodules are iron containing a small amount of titanium while the surrounding silicate is composed of iron, silicon, calcium, phosphorous, manganese, and small amounts of titanium, aluminum, and magnesium. The silicate particles observed on the typical fracture surfaces often show solidification structures in voids and dendritic structures as seen in Figures 12 and 13.

A piece of specimen 0404A, which exhibited internal corrosion on the fracture surface, was sectioned and polished on three orthogonal planes. These planes are designated as the face - normal to the thickness of the test specimen, longitudinal - normal to the length, and transverse - normal to the width. Microhardness tests were performed on the polished surfaces. For the metal matrix the Vickers hardness is about $HV\ 111-164\ \text{kg/mm}^2$ ($R_B\ 66-85$) using a 100g (0.220 pound) weight. The higher values were observed for the face section, intermediate values for the transverse section, and the lower values for the longitudinal section although there was some overlap. The inclusions are much harder. Values for the inclusions ranged from $HV\ 542-772\ \text{kg/mm}^2$ ($R_C\ 50-60$) with one value of $HV\ 217\ \text{kg/mm}^2$ ($R_B\ 96$).

A typical magnified image from the face section obtained by an optical metallograph is shown in Figure 14. The inclusions have two types of composition as indicated by electron/x-ray spectrometry of this polished surface. Some smaller inclusions are composed of iron and silicon with small amounts of phosphorous and titanium. Some larger inclusions have a dendritic or spherical phase surrounded by another phase. This surrounding phase is composed of iron, silicon, calcium, phosphorous, sulfur, titanium, manganese, aluminum, and magnesium; while the inner phase is composed of the same elements but has less calcium, slightly less manganese, more sulfur, and somewhat more titanium.

On the face section the inclusions have irregular shapes but they are roughly equiaxed. On the longitudinal and transverse sections, shown in Figures 15 and 16 respectively, the larger inclusions are long and thin and so they are platelets while the smaller inclusions are equiaxed and so they are roughly spherical. On both the transverse and longitudinal sections an occasional large inclusion will be equiaxed indicating a large particle.

Projections of the water temperature at the site of the wreck indicate an annual variation from 284K (52F) to 293K (68F). A low temperature ductile-to-brittle

transition, if it occurred between the temperature of the wreck and the temperature at which the mechanical properties were determined, about 297K (75F), would cause the wreck to be much more fragile than the tensile tests indicated. To determine whether the wreck would remain ductile at the temperature of the seawater, two notch impact tests were performed at about 77K (-321F) and 273K (32F). The specimen struck at 77K broke in a brittle manner and the fracture surface had large, shiny facets. Figure 17 is a scanning electron micrograph of this surface showing the facets and river markings characteristic of brittle cleavage. The specimen struck at 273K behaved in a ductile manner, requiring much more energy to cause fracture. The fracture surface appeared woody like those in the tensile tests. Figure 18 is a representative micrograph of this fracture surface.

Another specimen, 0405B, was subjected to a bend-fatigue test. Although the maximum initially applied stress was roughly equal to the yield strength, the stress decayed to much less than the yield strength during the beginning of the test and so the specimen did not break after three million cycles of low deflection-amplitude testing. The test machine was adjusted to produce reversed bending at a higher amplitude and the specimen broke at 0.2 million cycles. These results suggest that the material is susceptible to creep and may not fatigue harden significantly.

In conclusion, the results of the tensile tests indicate that the USS Monitor hull plate has strength similar to that of modern wrought iron except in the case of the specimen which showed severe internal corrosion. This strength is such that a square millimeter will support more than 180 newtons (26,000 pounds per square inch) of perpendicular load without deforming. Due to the low ductility observed, bending of the metal plates should be avoided. A consideration that must be made is that the rust will not carry much load, so in critically loaded parts the cross-sectional area of the metal must be determined carefully. A more insidious difficulty is the presence of internal corrosion. This internal corrosion cannot be recognized until after failure. The results of the tensile test of specimen 0404A indicate that a safety factor of 1/2 may be adequate although other volumes of metal may be more severely corroded.

The locations of the tensile test specimens in the hull plate were such that specimens 0404 were perpendicular to specimens 0405. The lower strength and ductility observed in specimen 0404B when compared to specimens 0405A and 0405C may be due to the corrosion observed in 0404A affecting the adjacent specimen, 0404B, or it may be due to an anisotropy in the two directions. Comparison of Figures 15 and 16 as well as additional optical micrographs suggests that the silicate platelets are somewhat longer in the longitudinal direction of specimen 0404A than in the transverse direction. Scanning electron micrographs of the fracture surfaces also suggest that the longer axis of the silicate platelets are perpendicular to the tensile axis of 0404 and parallel to the tensile axis of 0405. In analogy with fiber reinforced composite materials one would expect more toughness when the tensile axis is parallel to the fiber axis. The strength and ductility reduction in 0404B is therefore consistent with the longer axes of the platelets being perpendicular to the tensile axis. This elongation of the platelets is probably due to directional anisotropy in processing of the metal. Since the anisotropy is difficult to observe in the wreck, the lower values of strength and ductility should be used as a guide.

The properties of this antique wrought iron are similar to those of lower grades of modern wrought iron. In the modern metal the silicate inclusions are found to be in the form of cylindrical fibers while in the metal of the USS Monitor the inclusions are in the form of spheres and platelets. This difference may be due to the use of multiple hot rolling for modern wrought iron and pressing and hammering for the antique wrought iron.

ACKNOWLEDGEMENT

The authors greatly acknowledge the assistance with research and production of this report by S. Bilodeau, E. Brooks, J. Chadbourne, J. DeVault, M. Hammer, T. Harrison, B. Heit, A. Kummer, S. McCoy, G. Peace, E. Pierpoint, and G. Porkert.

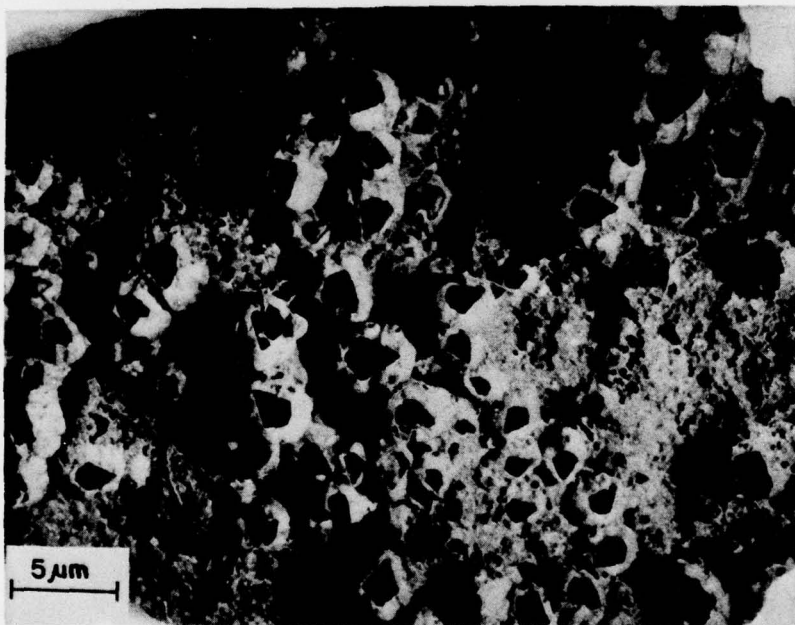


Fig. 1 — Piece of rust and accretion typical of that observed on surface of samples

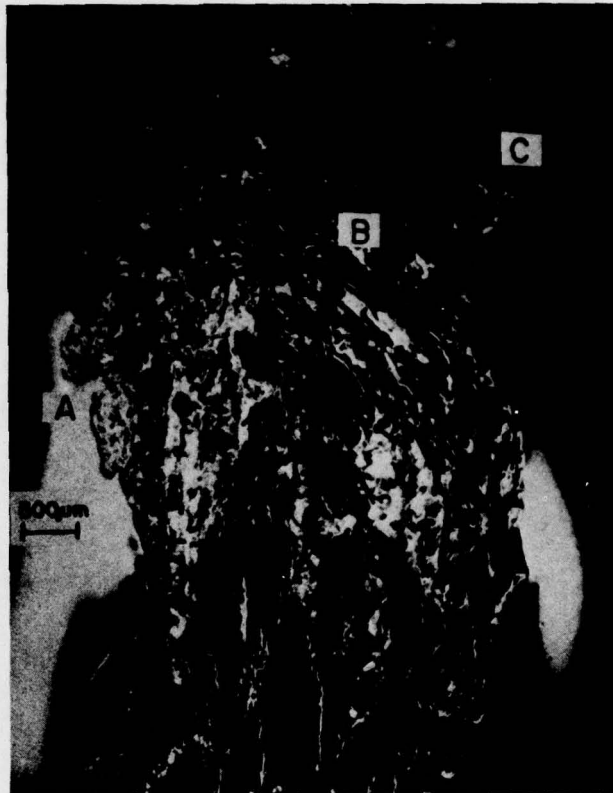


Fig. 2 — Optical micrograph showing rust (A), wax (B), and barnacles (C)



Fig. 3 — Optical micrograph showing two phase silicate particle embedded in rust

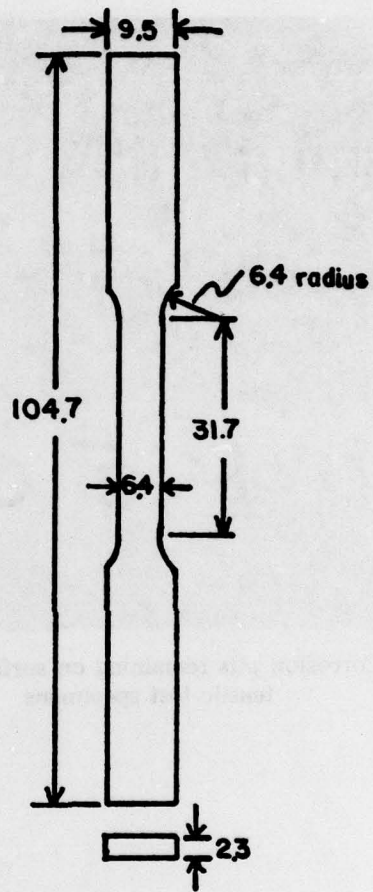


Fig. 4 — Dimensions of tensile test specimens in millimeters

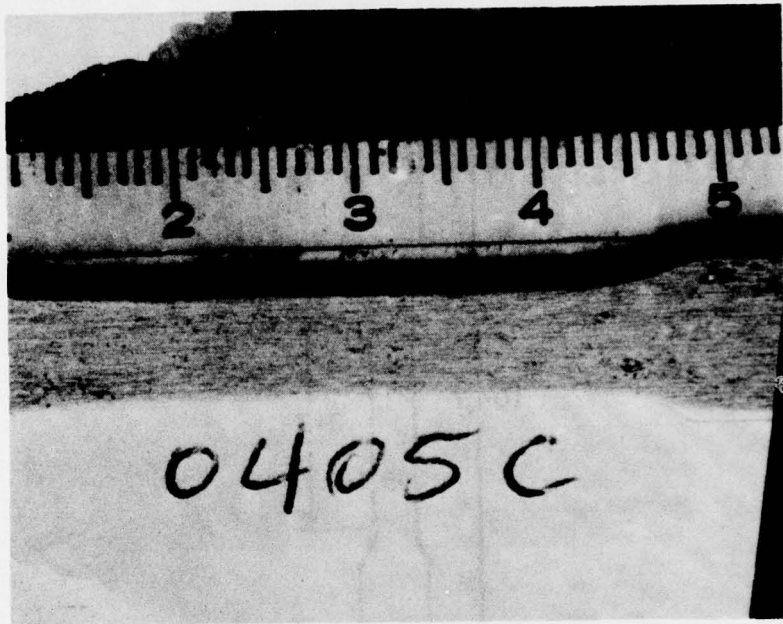


Fig. 5 — Corrosion pits remaining on surface of machined tensile test specimens

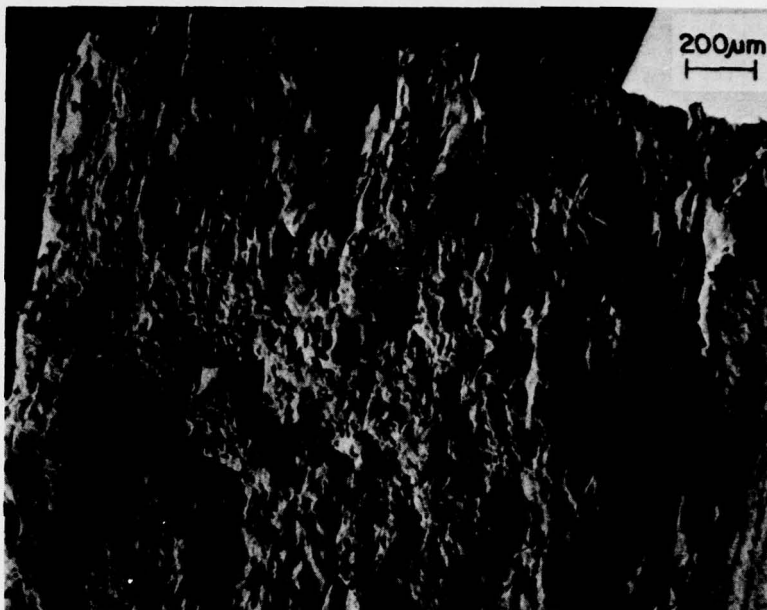


Fig. 6 — Woody fracture surface typical of wrought iron.
Specimen 0405A.

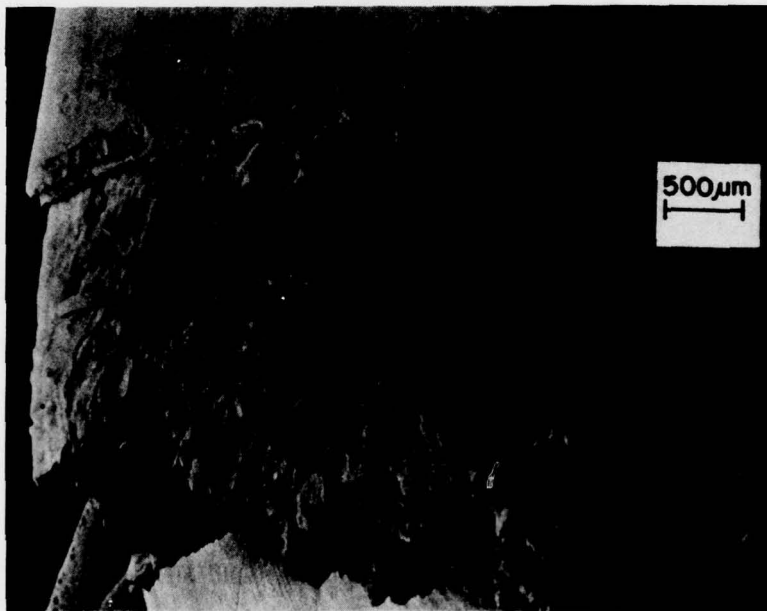


Fig. 7 — Delaminated surface resulting from internal corrosion.
Specimen 0404A.

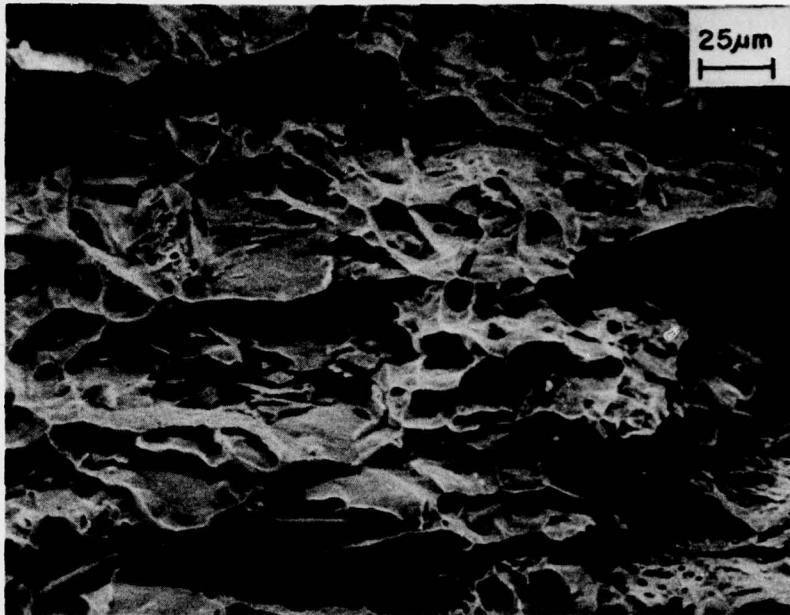


Fig. 8 — Typical fracture surface showing void formation around inclusion particles. Specimen 0405A.

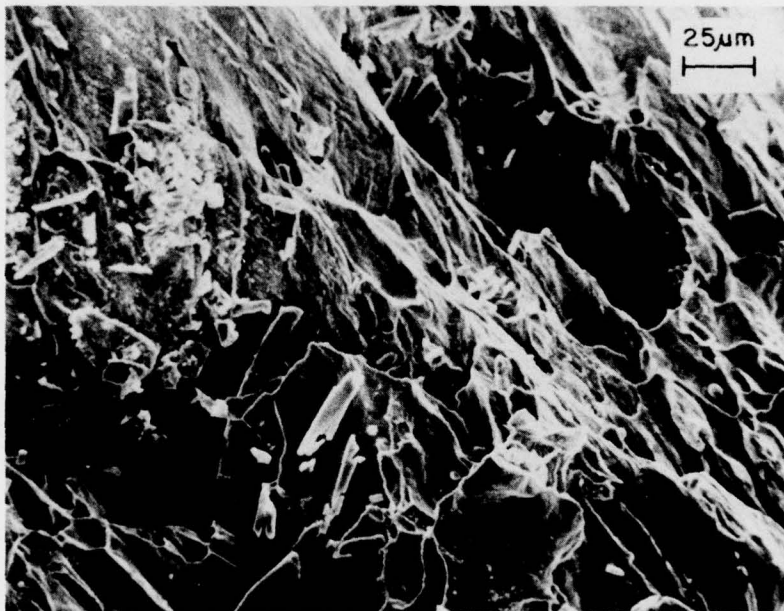


Fig. 9 — Typical fracture surface showing siliceous debris

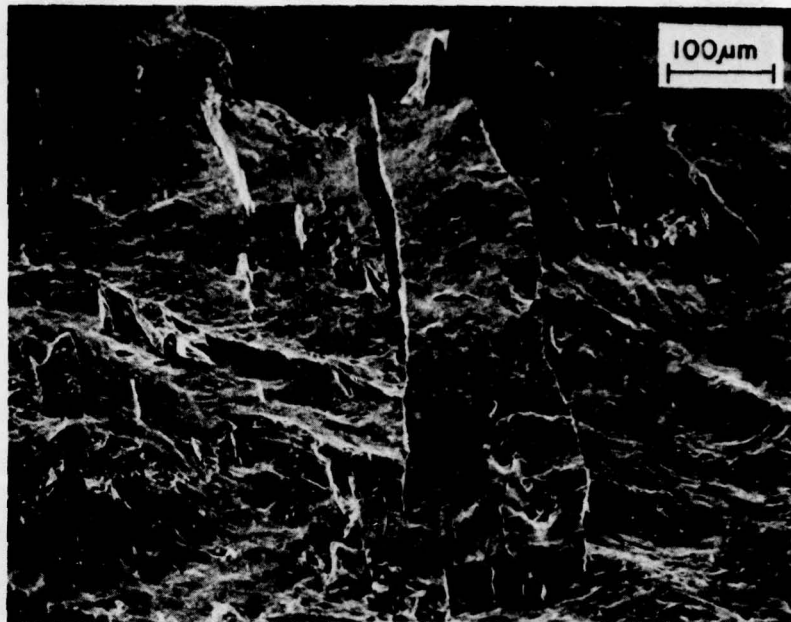


Fig. 10 — Large silicate platelets on delaminated surface.
Specimen 0404A.



Fig. 11 — Iron particles embedded in silicate platelet on delaminated surface. Higher magnification of Figure 10.

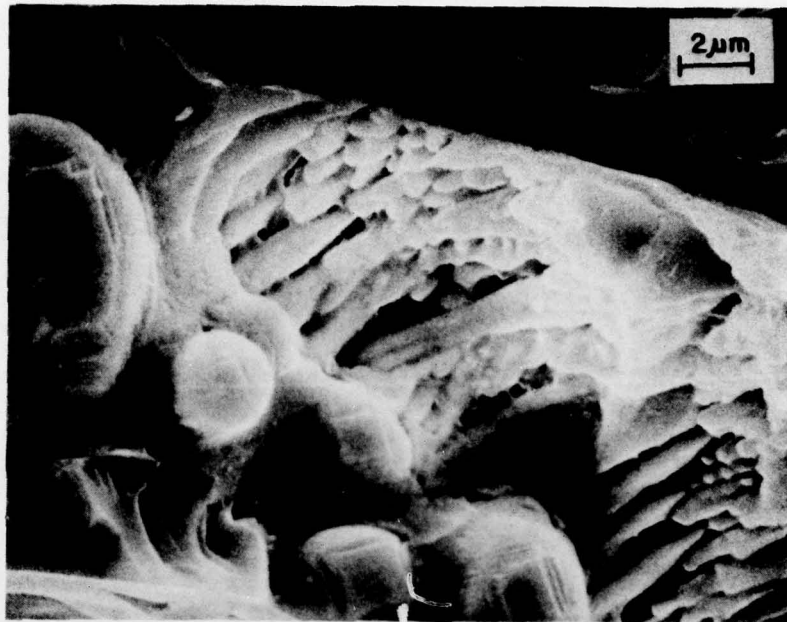


Fig. 12 — Faceted growth structures in siliceous void.
Specimen 0404B.

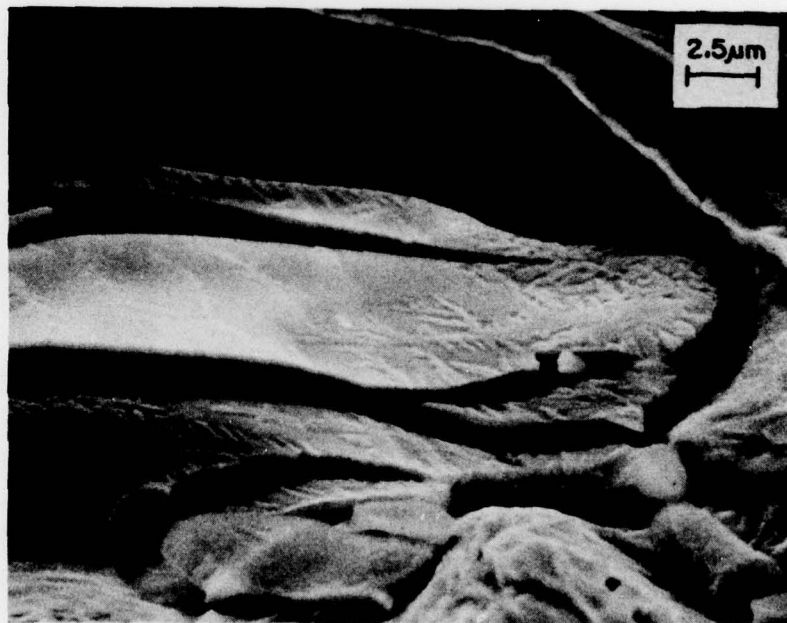


Fig. 13 — Dendritic second phase in silicate platelet.
Specimen 0405A.



**Fig. 14 — Optical micrograph of polished face section.
Specimen 0404A.**

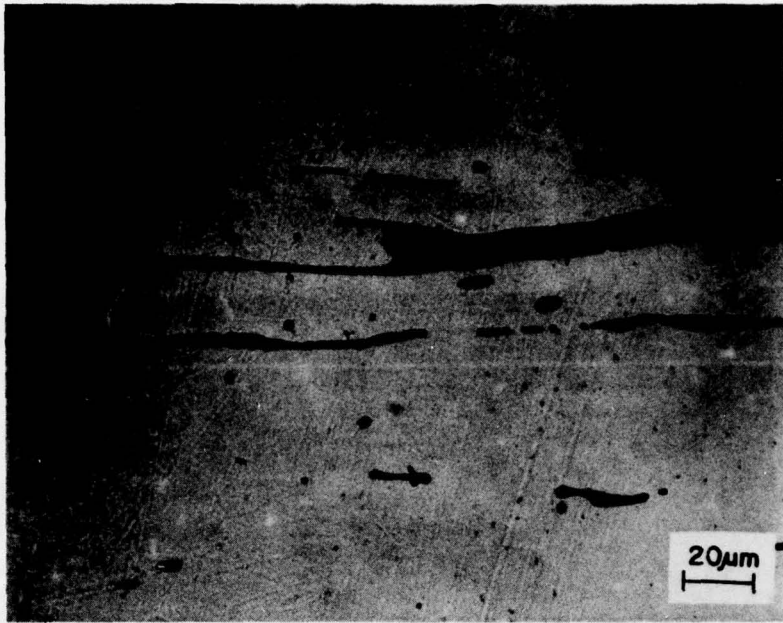


Fig. 15 — Optical micrograph of polished longitudinal section.
Specimen 0404A.

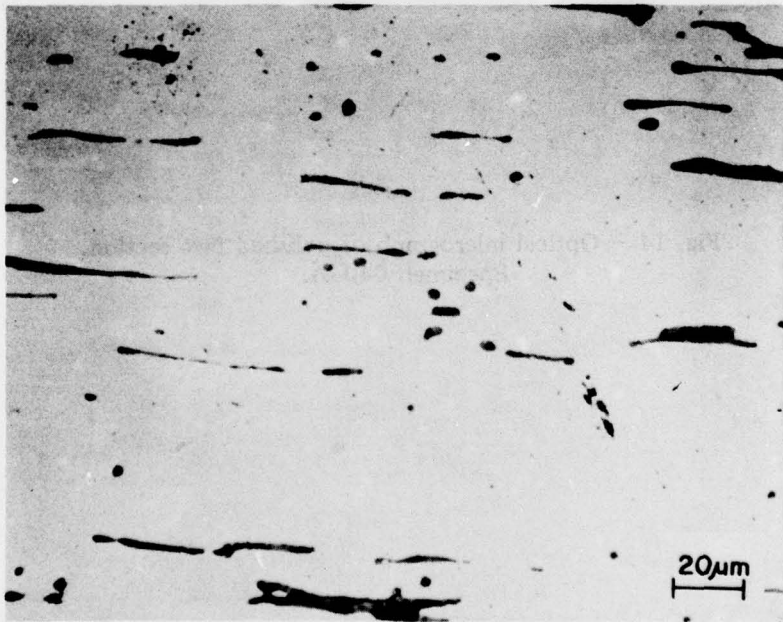


Fig. 16 — Optical micrograph of polished transverse section.
Specimen 0404A.

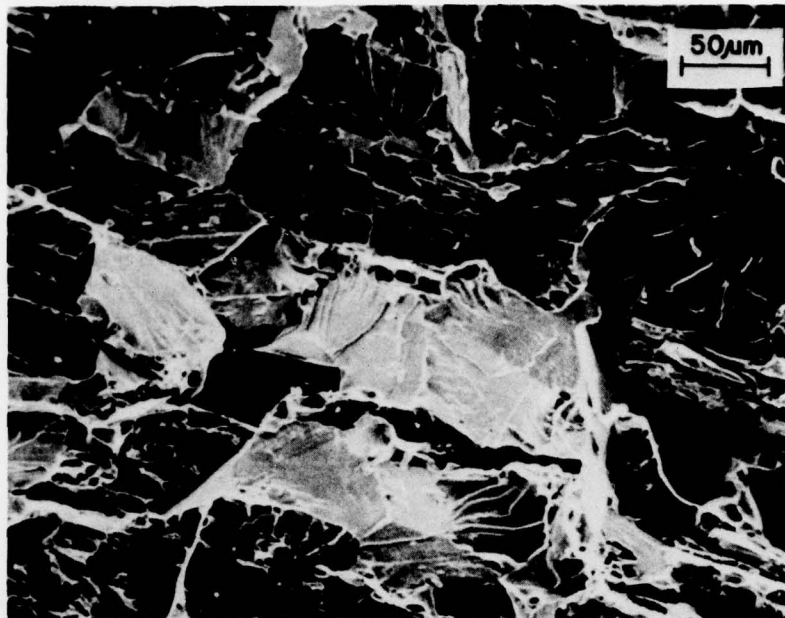


Fig. 17 — Brittle fracture surface of specimen fractured by impact at 77K (-321F). Specimen 0404C.

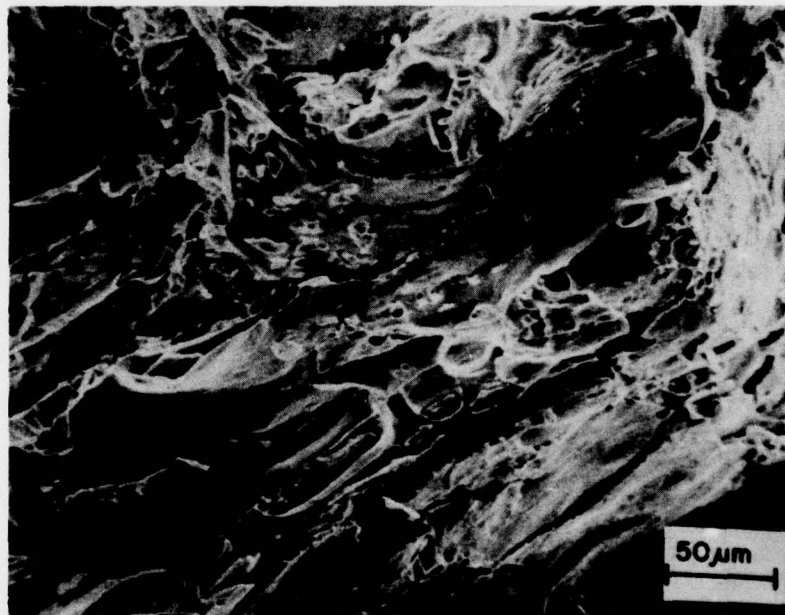


Fig. 18 — Ductile fracture surface of specimen fractured by impact at 273 K (32F). Specimen 0404B.